Accepted for publication in The Astrophysical Journal
Preprint typeset using LaTeX style emulateapj v. 12/16/11

THE DEPENDENCE OF CONVECTIVE CORE OVERSHOOTING ON STELLAR MASS: ADDITIONAL BINARY SYSTEMS AND IMPROVED CALIBRATION

Antonio Claret [1] and Guillermo Torres [2]

Accepted for publication in The Astrophysical Journal

ABSTRACT

Many current stellar evolution models assume some dependence of the strength of convective core overshooting on mass for stars more massive than 1.1–1.2 $M_\odot$, but the adopted shapes for that relation have remained somewhat arbitrary for lack of strong observational constraints. In previous work we compared stellar evolution models to well-measured eclipsing binaries to show that, when overshooting is implemented as a diffusive process, the fitted free parameter f_{ov} rises sharply up to about 2 $M_\odot$, and remains largely constant thereafter. Here we analyze a new sample of eight binaries selected to be in the critical mass range below 2 $M_\odot$ where f_{ov} is changing the most, nearly doubling the number of individual stars in this regime. This interval is important because the precise way in which f_{ov} changes determines the shape of isochrones in the turnoff region of ~1–5 Gyr clusters, and can thus affect their inferred ages. It also has a significant influence on estimates of stellar properties for exoplanet hosts, on stellar population synthesis, and on the detailed modeling of interior stellar structures, including the calculation of oscillation frequencies that are observable with asteroseismic techniques. We find that the derived f_{ov} values for our new sample are consistent with the trend defined by our earlier determinations, and strengthen the relation. This provides an opportunity for future series of models to test the new prescription, grounded on observations, against independent observations that may constrain overshooting in a different way.

Keywords: binaries: eclipsing; convection; stars: evolution; stars: interiors; stars: fundamental parameters

1. INTRODUCTION

Stars more massive than 1.1–1.2 $M_\odot$ develop convective cores and experience the phenomenon of core overshooting, which effectively enlarges this central region beyond the limits specified by the classical Schwarzschild criterion. Stellar models computed with convective core overshooting have longer main-sequence lifetimes, and have a higher degree of mass concentration toward the center. Such models have been quite successful at matching the measured physical properties (masses, radii, temperatures) of double-lined eclipsing binaries (DLEBs), and have also significantly improved the agreement between theory and observation regarding the measured rates of apsidal motion in eccentric DLEBs, compared to historical comparisons (see, e.g., Claret & Gim´enez 1993, 2010). Additional examples illustrating the need for convective core overshooting, mainly in the context of DLEBs, were given by Claret & Torres (2016) and references therein.

The last decade or so has seen renewed interest in the subject of overshooting with a number of efforts directed toward understanding the underlying physics, discriminating among various proposed mechanisms, constraining how much overshooting is needed, and establishing how it might vary as a function of the mass of the star (see Ribas et al. 2000; Claret 2007; Magic et al. 2010; Aerts 2013; Meng & Zhang 2014; Stancliffe et al. 2015; Valle et al. 2016; Moravveji et al. 2016; Deheuvels et al. 2016; Pedersen et al. 2018). A brief historical overview may be found in our earlier papers in this series, Claret & Torres (2016) (Paper I) and Claret & Torres (2017) (Paper II).

The most recent of these studies used a sample of 29 well-measured DLEBs to investigate the dependence of core overshooting on stellar mass in the framework of the increasingly popular diffusive approximation, with its free parameter f_{ov} that controls the extent of the overshooting layer (Freytag et al. 1996; Herwig et al. 1997; see also Section 3 for the mathematical definition of f_{ov}). It was found that f_{ov} increases rapidly in the range between ~1.2 and ~2.0 $M_\odot$ from a value of zero to about 0.016, and changes little thereafter, up to the 4.4 $M_\odot$ mass limit of the observational sample. This result was found to be independent of the adopted (solar-scaled) element mixture (Grevesse & Sauval 1998, or Asplund et al. 2009), even though the first choice was used in combination with a different primordial helium abundance and enrichment law than the second. Related to this, Paper II also showed that, regardless of the element mixture, the fractional change in the mass of the convective core at the zero-age main-sequence (ZAMS) compared to standard (i.e., no-overshooting) models has a steeper dependence on mass for less massive stars, leveling off beyond about 2 $M_\odot$. The trend is connected with the opacities, the equation of state, and the nuclear reaction rates.

The importance of the above study is that it provided the first reasonably well-established semi-empirical calibration of f_{ov} as a function of stellar mass, at least up to 4.4 $M_\odot$. Prior to that work, most publicly available grids of stellar evolution calculations used somewhat arbitrary prescriptions to describe the change in the efficiency of

[1] Instituto de Astrof´ısica de Andaluc´ıa, CSIC, Apartado 3004, 18080 Granada, Spain
[2] Harvard-Smithsonian Center for Astrophysics, 60 Garden St., Cambridge, MA 02138, USA

overshooting with mass, or even a constant value for f_{ov} regardless of the mass of the star.

A weakness of the calibration of f_{ov} with mass in Paper II, however, is the shortage of stars in the critical mass range below about 2 $M_\odot$, seen in Figure 2 of that work. This is where overshooting is changing the most. The way in which f_{ov} varies as a function of mass can have considerable impact on the morphology of isochrones constructed from evolutionary tracks, and nowhere is this detailed shape more important than at the turnoff of open clusters. This region of a cluster's color-magnitude diagram carries most of the weight for determining its age from classical isochrone fits. Turnoff masses in the ~1.2–2.0 $M_\odot$ interval correspond to cluster ages roughly in the range 1–5 Gyr, which encompasses a large fraction of the well-known and best-studied open clusters in the Milky Way. The impact of overshooting extends to many other fields including population synthesis, the determination of stellar properties for exoplanet hosts larger than about 1.2 $M_\odot$, and the calculation of oscillation frequencies that can be measured with asteroseismic techniques. Indeed, these measurements already exist for large numbers of stars based on observations from space missions such as CoRoT, Kepler/K2, and soon others such as TESS and PLATO. A first motivation for the present paper is therefore to enlarge the sample of DLEBs in this critical mass interval in order to improve the definition of the slope. To this end we examined the literature and identified seven systems with well-measured properties that might be added and that are all on the main-sequence, some reaching near the terminal-age main sequence (TAMS) where sensitivity to overshooting is greater. We refer to this as our "main sample".

Coincidentally, all seven binaries have previously been reported to be problematic to fit with current models, in the sense that the more massive primary components were found to be systematically younger than the secondaries (Clausen et al. 2010; Torres et al. 2014). In light of the way in which the strength of overshooting is now known to change with stellar mass precisely in the mass range of these binaries, our suspicion is that this may play an important role in those difficulties. Resolving this lingering issue provides an additional motivation for our study.

Thirdly, two other classical systems, YZ Cas and TZ For, are of particular interest and may be added as well. YZ Cas is a moderately evolved system with components of very different mass (2.26 and 1.32 $M_\odot$), one of which is in the range we are most concerned with here. The unequal masses provide increased leverage for testing models, and a unique opportunity to examine the f_{ov} vs. mass relation within the same system. Previous studies have concluded that current models are unable to match all measured properties simultaneously (Pavlovski et al. 2014). TZ For is a rare example of a binary with one component in the helium-burning phase and the other less evolved, which has had its absolute masses significantly improved recently (Gallenne et al. 2016). Both stars are near 2 $M_\odot$, precisely where the overshooting relation appears to turn over.

Lastly, we take the opportunity to improve our previous fit and inferred f_{ov} values in Paper II for the evolved eclipsing system OGLE-LMC-ECL-15260, a pair of giants with indistinguishable masses around 1.4 $M_\odot$ but very different sizes, and to correct a misprint for OGLE-LMC-ECL-03160 in Table 2 of that work.

The layout of our paper is as follows. Section 2 introduces our new sample of DLEBs. In Section 3 we describe the stellar evolution codes employed, and the methodology we use to infer the values of f_{ov} and the mixing length parameter α_{MLT} for each star in each system. The results are then reported and discussed in Section 4 based on calculations with two different element mixtures, and the last section presents our concluding remarks.

2. BINARY SYSTEMS

The sample of objects for this study is designed to strengthen the calibration of f_{ov} vs. mass in the important but sparsely populated regime under about 2 $M_\odot$, which has the steepest slope. Initially we selected a total of nine DLEBs not included in Paper II that have well measured masses and radii with relative uncertainties formally smaller than 3%, as well as measured effective temperatures and in most cases also spectroscopic metallicities. All are near the solar abundance, and are evolved enough that their properties are sufficiently sensitive to the effects of overshooting. Seven of these systems (V442 Cyg, GX Gem, BW Aqr, AQ Ser, BF Dra, BK Peg, and CO And) contain main sequence components of similar masses ($q \equiv M_2/M_1 \gtrsim 0.9$) and have been challenging to fit with models in the past, as mentioned in the Introduction. We are now able to match all of their properties well except for AQ Ser, which remains problematic. We discuss our attempts to fit this system later, but have chosen to exclude it from our investigation of the dependence of f_{ov} with mass.

The final two systems are TZ For, in which the primary is a giant, and YZ Cas, with components of very different masses ($q = 0.59$) on either side of the 2 $M_\odot$ threshold at which the f_{ov} relation changes slope. The mass determinations for TZ For have been revised by Gallenne et al. (2016) based on new spectroscopic and interferometric observations since the original study by Andersen et al. (1991), and while the uncertainties are significantly improved, the mass values are not very different from the previous ones. Gallenne et al. (2016) kept the original radii from Andersen et al. (1991), as their study did not include new light curves. We have made slight adjustments to the radii here, to account for the fact that the semimajor axis of the binary changed slightly with the new spectroscopic observations.

The properties of the all systems and the sources for the adopted values are collected in Table 1, in order of decreasing primary mass. The eight binaries we retain for this study (i.e., all except for AQ Ser) represent a 28% increase over the sample size considered in Paper II. In addition to these eight binaries, we have revisited OGLE-LMC-ECL-15260 using the same physical properties given in our earlier study.

3. MODELS AND METHODS

The principal results for f_{ov} reported in this paper are based on calculations with the Modules for Experiments in Stellar Astrophysics package (MESA; Paxton et al. 2011, 2013, 2015), version 7385. Microscopic diffusion was included (even for the more massive of our binaries, including TZ For) as it is an important process in the

Table 1
Binaries systems in our sample.

Name	Mass ($M_\odot$)	Radius ($R_\odot$)	$T_{\rm eff}$ (K)	[Fe/H]	Source
YZ Cas	2.263 ± 0.012	2.525 ± 0.011	9520 ± 120	+0.01 ± 0.11	1
	1.325 ± 0.007	1.331 ± 0.006	6880 ± 240		
TZ For	2.057 ± 0.001	8.34 ± 0.12	4930 ± 100	+0.01 ± 0.04	2,3,4
	1.958 ± 0.001	3.97 ± 0.09	6650 ± 200		
V442 Cyg	1.560 ± 0.024	2.073 ± 0.034	6900 ± 100		4,5
	1.407 ± 0.023	1.663 ± 0.033	6800 ± 100		
GX Gem	1.488 ± 0.011	2.326 ± 0.012	6195 ± 100	−0.12 ± 0.10	4,6
	1.467 ± 0.010	2.236 ± 0.012	6165 ± 100		
BW Aqr	1.479 ± 0.019	2.062 ± 0.044	6350 ± 100	−0.07 ± 0.11	4,7,8
	1.377 ± 0.021	1.786 ± 0.043	6450 ± 100		
AQ Ser	1.417 ± 0.021	2.451 ± 0.027	6340 ± 100		9
	1.346 ± 0.024	2.281 ± 0.014	6430 ± 100		
BF Dra	1.414 ± 0.003	2.086 ± 0.012	6360 ± 150	−0.03 ± 0.15	10
	1.375 ± 0.003	1.922 ± 0.012	6400 ± 150		
BK Peg	1.414 ± 0.007	1.988 ± 0.008	6265 ± 85	−0.12 ± 0.07	8
	1.257 ± 0.005	1.474 ± 0.017	6320 ± 90		
CO And	1.2892 ± 0.0073	1.727 ± 0.021	6140 ± 130	+0.01 ± 0.15	11
	1.2643 ± 0.0073	1.694 ± 0.017	6170 ± 130		

Note. — The first line for each system corresponds to the more evolved star. In some cases we list Torres et al. (2010) as an additional source, as the original determinations were slightly revised in that work through the use of updated physical constants. The [Fe/H] value for YZ Cas is that of the secondary; the primary is an Am star. The [Fe/H] value for TZ For is the weighted average for the primary and secondary, and the radii have been updated for this work as described in the text. Sources are: (1) Pavlovski et al. (2014); (2) Andersen et al. (1991); (3) Gallenne et al. (2016); (4) Torres et al. (2010); (5) Lacy & Frueh (1987); (6) Lacy et al. (2008); (7) Clausen (1991); (8) Clausen et al. (2010); (9) Torres et al. (2014); (10) Lacy et al. (2012); (11) Lacy et al. (2010).

mass range of the present sample. Rotation was not considered, and mass loss (only relevant for TZ For) was taken into account following Reimers (1977), with an efficiency coefficient of $\eta = 0.2$. Convective core overshooting was treated in the diffusive approximation, characterized by the free parameter f_{ov}. Following Freytag et al. (1996) and Herwig et al. (1997) the diffusion coefficient in the overshooting region is given by

$$D_{ov} = D_0 \exp\left(\frac{-2z}{H_v}\right), \qquad (1)$$

where D_0 is the diffusion coefficient at the convective boundary, z is the geometric distance from the edge of the convective zone, H_v is the velocity scale height at the convective boundary expressed as $H_v = f_{ov} H_p$, and the coefficient f_{ov} governs the width of the overshooting layer. The symbol H_p corresponds to the pressure scale height at the edge of the convective core. The temperature gradient in this region is assumed to be radiative, and equal values of f_{ov} were adopted above the hydrogen- and helium-burning regions.

For comparison purposes, the analysis was carried out using the two most common element mixtures for the opacities, by Grevesse & Sauval (1998) (GS98), and Asplund et al. (2009) (A09). In both cases we adopted a primordial helium abundance of $Y_p = 0.249$ (Planck Collaboration 2016) along with a slope for the enrichment law of $\Delta Y/\Delta Z = 1.67$, unless otherwise indicated. For stars with convective envelopes we used the standard mixing-length theory (Böhm-Vitense 1958) with its usual free parameter $\alpha_{\rm MLT}$. Although in what follows $\alpha_{\rm MLT}$ is adjusted independently for each star, we note for reference that its value calibrated against the Sun with these models is $\alpha_{\rm MLT} = 1.84$ for the A09 mixture (see Torres et al. 2015). The third-degree equation relating the temperature gradients was solved using the Henyey option in MESA, and for the condition to set the boundary of the convection zone we adopted the Schwarzschild criterion.

A second set of models based on the Granada evolutionary code (Claret 2004) was used both to check for consistency with a completely independent code, and to perform further tests on some of the less satisfactory fits with MESA. Diffusion was not considered, as it is not implemented in the Granada code, and convective core overshooting follows the classical step-function formulation, rather than the diffusive approximation we used in MESA. In the classical prescription the extra distance traveled by convective elements beyond the boundary of the core is given by $d_{ov} = \alpha_{ov} H_p$, with α_{ov} being a free parameter. In Paper II we showed that there is a fairly tight correlation between α_{ov} and f_{ov} such that $\alpha_{ov}/f_{ov} \approx 11.36 \pm 0.22$. We use this below as a handy conversion factor between the two overshooting parameters when comparing results from the MESA and Granada codes.

For both models the calculations were performed starting from the pre-main-sequence phase, and in the case of TZ For with its giant primary component, they were extended up to the helium-burning phase. Extensive grids of evolutionary tracks for the measured mass of each binary component were generated for f_{ov} values ranging from 0.000 to 0.025 in steps of 0.002 with MESA, and α_{ov} values of 0.00–0.25 with the Granada code, in steps of 0.02. Mixing length values in both cases ranged between $\alpha_{\rm MLT} = 1.2$ and 2.4, with a resolution of 0.1. For systems that we found to require it we occasionally ex-

tended the α_{MLT} dimension up to a value of 2.7. In most cases the chemical abundance of the binaries has been measured, and the grids adopted those values. In other cases it was not known, or was uncertain, or was simply based on fits to stellar evolution models by others, and additional values were tried.

Our fitting procedure is essentially the same as used in Paper II, and the reader is referred to that work for the details. Briefly, the observational constraints for each star are the masses, radii, and effective temperatures. A best match to each point in the grid was sought using a simple χ^2 statistic to infer the optimal values of f_{ov} (or α_{ov} for the Granada tracks) and α_{MLT}, with the initial metal abundance Z constrained to be the same for the two stars in each binary. After verifying that the preferred matches were similar between MESA and Granada (accounting for the scaling between α_{ov} and f_{ov}), and that the implied evolutionary states were also the same, we then computed finer MESA grids tailored to each system and manually fine-tuned the overshooting and mixing length parameters (often varying Z as well) to obtain the final best fits. Throughout this procedure we required that the ages be the same for the components within 5%, to allow for imperfections in the models. We found satisfactory fits for all eight of our targets, and the special case of the AQ Ser system that we have excluded will be discussed later. Typical (1σ) uncertainties for the inferred f_{ov} values are estimated to be 0.004 (0.003 for the giant component of TZ For, whose more advanced state makes it more sensitive to overshooting), and 0.20 for α_{MLT}. These were determined through experiments in which we varied one parameter at a time while requiring the predicted radii and temperatures of the stars to be within their observational uncertainties, and the ages to be consistent within 5%, and also by examining our grids (in which all parameters were varied) in the vicinity of the best-fit values, again requiring agreement with the observations.

4. RESULTS AND DISCUSSION

4.1. V442 Cyg, GX Gem, BW Aqr, BF Dra, BK Peg, and CO And

The inferred values of f_{ov} and α_{MLT} from our best fits are presented for all our targets in Table 2, for both the GS98 and A09 mixtures[3]. There are only minor differences in the derived parameters between the two sets, which are well within the uncertainties. Also listed are the best-fit initial abundances, Z. Both sets of fitted Z values are in good agreement with the measured metallicities within their uncertainties, once due account is taken of the effects of element diffusion, which tends to decrease the surface abundance through gravitational settling of heavy elements (Michaud 1970; Michaud et al. 1976; Dotter et al. 2017). As expected, the abundances derived with the GS98 mixture are typically larger than the ones that use A09, consistent with fact that the corresponding solar abundances are different. The mean ages, given in the last column, are systematically older for A09. Best fits to four of our targets are illustrated in Figure 1.

[3] We include OGLE-LMC-ECL-03160 in the table, to report a correction to the GS98 value of f_{ov} for the primary of the system that was misprinted in Table 2 of Paper II.

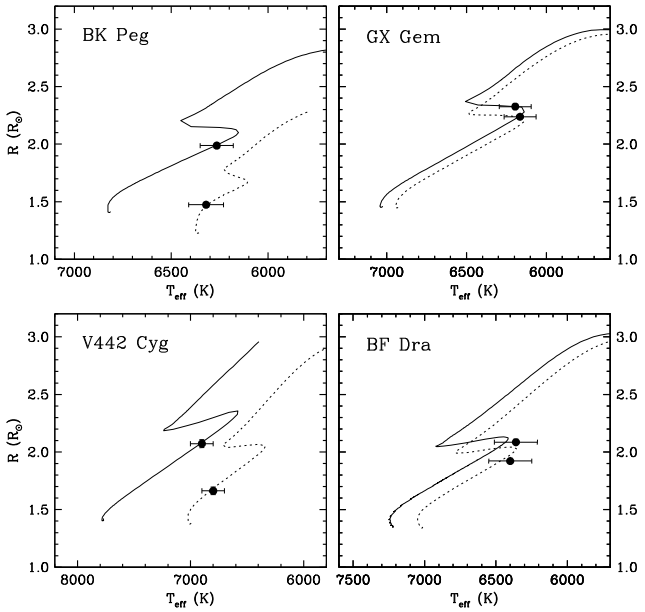

Figure 1. Four sample fits to evolutionary tracks from the MESA models using the A09 mixture (solid lines for the primary, dotted for the secondary). The corresponding model parameters are listed in Table 2.

As indicated earlier, in the past it has not been possible to achieve entirely satisfactory matches to the physical properties of any of our seven main targets (V442 Cyg, GX Gem, BW Aqr, AQ Ser, BF Dra, BK Peg, and CO And) with current models unless the primaries are permitted to be significantly younger than the secondaries, sometimes by as much as 15%. In most cases those fits were carried out with the same amount of core overshooting for the two components, often a fairly high value such as $\alpha_{ov} \approx 0.20$ or $f_{ov} \approx 0.020$. Interestingly, by now allowing the strength of the overshooting to be different for each star, we have succeeded in matching all of their properties to well within the measurement uncertainties, at nearly the same age for the two components. The only exception is AQ Ser, which we discuss separately below. The masses of all these binaries happen to lie in a critical regime of the overshooting calibration curve reported in Paper II, where f_{ov} is not only smaller than mentioned above, but is also changing rapidly so that even a small difference in mass can result in a sizable difference in the inferred age of a star when the behavior of f_{ov} is properly taken into account.

A graphical representation of our inferred f_{ov} values for each star as a function of stellar mass for the A09 mixture (filled circles) is shown in Figure 2 see below for a description of the curve overdrawn), along with the measurements for the 29 other DLEBs reported by Claret & Torres (2017) in Paper II that were derived with the same element mixture and helium abundance (open squares), and the same methodology. We include in the figure our determinations for the more massive binaries YZ Cas and TZ For as well (see below). The new measurements support the general trend found in Paper II, and are seen to complement that sample by filling in some of the gaps in the rising part of the relation. There appears to be one outlier (the primary component of BW Aqr) for which we infer a slightly larger f_{ov} value with the A09 mixture than with the

Table 2
Fitted overshooting and mixing length parameters using the GS98 and A09 mixtures.

Name	Primary f_{ov}	Primary α_{MLT}	Secondary f_{ov}	Secondary α_{MLT}	Z [a]	Mean age (Myr)
Grevesse & Sauval (1998) element mixture						
YZ Cas	0.016	2.00	0.006	2.74	0.012	492
YZ Cas [b]	0.0176	1.66	0.0035	1.66	0.012	522
TZ For	0.018	1.95	0.017	2.10	0.020	1114
V442 Cyg	0.004	1.90	0.003	1.90	0.014	1409
GX Gem	0.010	1.90	0.006	1.85	0.021	2349
BW Aqr	0.010	2.10	0.004	1.80	0.021	2062
BF Dra	0.008	1.95	0.005	1.85	0.014	2252
BK Peg	0.008	1.90	0.002	2.05	0.018	2244
CO And	0.003	1.93	0.000	1.72	0.016	2907
OGLE-LMC-ECL-15260 [c]	0.004	2.03	0.004	2.11	0.006	2249
OGLE-LMC-ECL-03160 [d]	0.008	1.94	0.008	2.15	0.0025	1023
Asplund et al. (2009) element mixture						
YZ Cas	0.015	1.70	0.005	2.67	0.010	525
YZ Cas [b]	0.0176	1.66	0.0035	1.60	0.010	556
TZ For	0.017	1.91	0.015	1.85	0.015	1131
V442 Cyg	0.004	1.90	0.003	1.90	0.012	1482
GX Gem	0.010	1.90	0.006	1.83	0.017	2397
BW Aqr	0.012	1.85	0.004	1.70	0.018	2108
BF Dra	0.008	1.95	0.005	1.80	0.010	2204
BK Peg	0.008	1.90	0.000	2.03	0.015	2311
CO And	0.002	1.90	0.000	1.72	0.014	3031
OGLE-LMC-ECL-15260 [c]	0.004	2.08	0.004	2.08	0.004	2138

Note. — Typical uncertainties are 0.004 for f_{ov} (0.003 for the giant primary of TZ For and both components of OGLE-LMC-ECL-15260) and 0.20 for α_{MLT}.

[a] Bulk (initial) composition.

[b] Preferred parameters, derived using the Granada code (Claret 2004) with the step-function approximation for overshooting rather than the diffusive approximation, and transforming α_{ov} to f_{ov} using the scale factor $\alpha_{ov}/f_{ov} = 11.36$ (see text). Values are given to one additional decimal place due to the conversion.

[c] Parameters from revised fits that supersede those reported in Claret & Torres (2017), and place the components in the blue loop rather than on the ascending giant branch (see text).

[d] The parameters listed here correct a misprint in Table 2 by Claret & Torres (2017) (Paper II) in the f_{ov} value for the primary. Note that the helium content for this determination is the one adopted in that work, based on $Y_p = 0.24$ and $\Delta Y/\Delta Z = 2.0$, rather than the one used here, although this has little influence on f_{ov}.

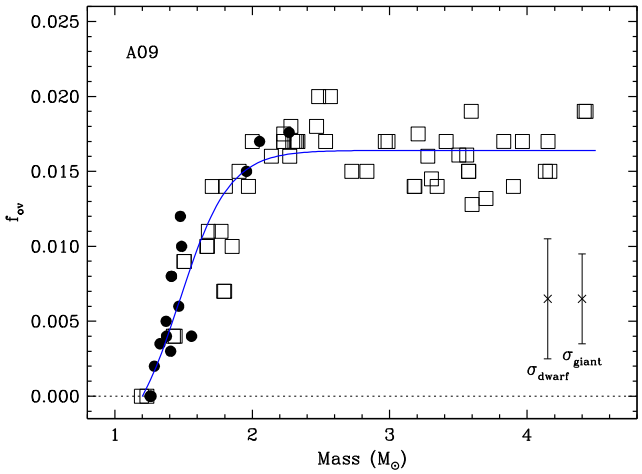

Figure 2. Inferred f_{ov} values from MESA models using the A09 mixture (Table 2) as a function of stellar mass. Filled circles represent the stars in the present sample (including YZ Cas and TZ For), and open squares are values taken for the 29 dwarf and giant DLEBs from Table 3 of Claret & Torres (2017), determined in the same way with the same element mixture and helium content. Typical error bars for dwarfs and giants are indicated on the lower right.

GS98 one, although the difference is well within our error bar. This star is also largely responsible for the hint of a somewhat steeper slope suggested by the current sample compared to that indicated by the few systems in Paper II below 2 $M_\odot$, though again, we do not consider this hint very compelling given the uncertainties. Additional, well-measured DLEBs in the 1–2 $M_\odot$ range are needed to investigate this possibility further.

At the suggestion of the referee we have drawn a curve in Figure 2 that provides a reasonable representation of the f_{ov} measurements.We constrained it by eye to start at 1.2 $M_\odot$ and to level off at a value given by the average f_{ov} of all stars with masses above 2 $M_\odot$, which is 0.0164. The expression used is

$$f_{ov} = \frac{0.02013}{1 + e^{-5.5(M-1.47)}} - 0.00373. \qquad (2)$$

We stress that there is no physical basis for this formula, which is intended solely to provide a convenient expression for the overshooting parameter as a function of stellar mass with relatively few parameters.

4.1.1. AQ Ser

For the AQ Ser system we were not able to obtain a satisfactory fit to its measured properties within our 5% cap for the age difference between the components, either with MESA or using the Granada code. With MESA we explored a wide range of chemical compositions (which is unconstrained observationally) and broader ranges in f_{ov}

and α_{MLT} than for our other binaries, for both element mixtures. We also performed fits using the temperature ratio as an observable rather than the absolute temperatures of the stars, on the premise that it is less prone to systematics in DLEB analyses because it does not depend as strongly on external calibrations, and because it is more closely tied than the absolute temperatures to the directly observable difference in eclipse depths. None of these attempts were successful. We did find an acceptable fit by arbitrarily increasing the secondary mass; the change required was about twice the observational error. An additional test with the Granada code involved using the same metallicity Z for both components, but not forcing the helium content to be same. This again gave a tolerably good fit, but at the price of requiring a difference ΔY of the order of 10% between the stars, which would seem unrealistically large.

While this failure of the models could suggest a measurement error in one or more of the physical properties of the stars (M, R, or T_{eff}), other causes cannot be ruled out. We note, for example, that the projected rotational velocity of the primary of AQ Ser is quite rapid ($v \sin i = 73 \pm 10$ km s^{-1}; Torres et al. 2014), while the primaries of both BK Peg and BF Dra have virtually identical masses as the primary of AQ Ser to within 0.2%, but have much slower projected rotational velocities of 16.6 ± 0.2 km s^{-1} and 10.5 ± 1.8 km s^{-1}, respectively (Clausen et al. 2010; Lacy et al. 2012). This occurs because of tidal synchronization, with the orbital period of AQ Ser being much shorter (1.69 days) than those of the other two binaries (5.49 and 11.21 days). It is possible that this relatively high rate of rotation in AQ Ser A (shared by the secondary, with $v \sin i = 59 \pm 10$ km s^{-1}) may have some effect on the evolution of the system, moving it away from the canonical evolution the stars would have if they were single.

4.2. TZ For and YZ Cas

TZ For is a DLEB with well-determined absolute dimensions in an advanced stage of evolution that makes it useful for this study, and we have added it to our sample to strengthen the calibration of f_{ov} vs. stellar mass. It resembles the much brighter (non-eclipsing) α Aur binary in that the secondary is in a very rapid phase of evolution crossing the Hertzprung gap while the primary is in the helium-burning clump. It represents an interesting example of significant differential evolution in a system featuring components of similar mass close to 2 $M_{\odot}$. Gallenne et al. (2016) have recently revisited the mass determinations, which were subsequently used by Valle et al. (2017) together with the other binary properties for a comparison with two sets of evolutionary models, focusing on inferring the amount of convective core overshooting. One of their determinations used MESA and the same diffusive overshooting approximation adopted here with the same A09 mixture, but with other minor differences including a fixed solar-calibrated mixing length parameter of $\alpha_{MLT} = 1.74$, and the assumption that the components have identical f_{ov} values. They reported two different solutions, their preferred one giving an age of 1.10 ± 0.07 Gyr and $f_{ov} = 0.013$ with a helium abundance implying $\Delta Y/\Delta Z \approx 1.5$, and the other, poorer fit giving an age of 1.23 ± 0.03 Gyr and $f_{ov} = 0.025$ for $\Delta Y/\Delta Z \approx 1.0$.

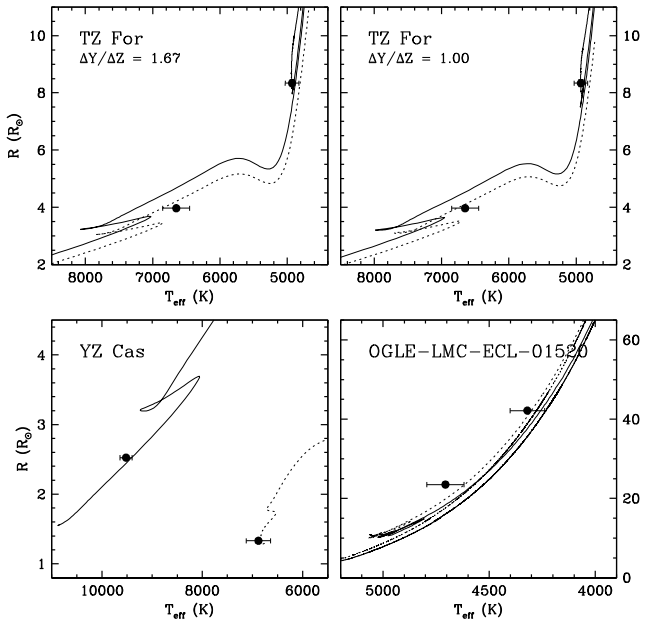

Figure 3. Top: Best-fit solutions with MESA for TZ For using two different enrichment laws ($\Delta Y/\Delta Z$) and the A09 mixture. Primary tracks are drawn with solid lines, secondary tracks with dotted lines. Differences are minor. Bottom: Best-fit solutions for YZ Cas using the Granada models and the step-function approximation to overshooting (A09 mixture), and for OGLE-LMC-ECL-15260 with MESA and the GS98 mixture, superseding the fit in Paper II that had the stars at a different evolutionary stage (see text). For both of these systems $Y_p = 0.249$ and $\Delta Y/\Delta Z = 1.67$.

Our own fits to TZ For with MESA give f_{ov} values intermediate between those above, and are reported in Table 2 for the GS98 and A09 mixtures and our adopted enrichment law ($Y_p = 0.249$, $\Delta Y/\Delta Z = 1.67$). Our mixing length parameters are slightly but not significantly super-solar, averaging $\alpha_{MLT} \approx 2.0$ for GS98 and $\alpha_{MLT} \approx 1.9$ for A09. To explore the robustness of these results we performed tests with a different enrichment law ($\Delta Y/\Delta Z = 1.0$) to match one of the fits by Valle et al. (2017), keeping Z fixed at our best-fit A09 value. We obtained essentially the same fits as with our standard enrichment law, leading also to the same position in the diagram of R vs. T_{eff} with the primary in the central helium-burning phase and the secondary on the subgiant branch (see top panels in Figure 3). This suggests f_{ov} is rather insensitive to the helium content, at least in this particular case.

The absolute properties of YZ Cas, another very interesting DLEB, were recently redetermined by Pavlovski et al. (2014) reaching a precision of 0.5% in the masses and radii of both components. The primary is a metallic-line A star ($M = 2.263$ $M_{\odot}$, A2m) that is significantly more massive than the normal, solar-composition secondary ($M = 1.325$ $M_{\odot}$, F2). The extreme mass ratio makes it a uniquely important object to study the dependence of overshooting as a function of mass within the same system, having one star on the flat part and the other on the rising part of the f_{ov} curve. Pavlovski et al. (2014) compared the measured properties of the system against several models, but reported difficulties finding a simultaneous match to all of the measurements. Their fits preferred a significantly lower metallicity than the one they measured for the secondary (taken to represent the bulk composition of the system, as the primary is

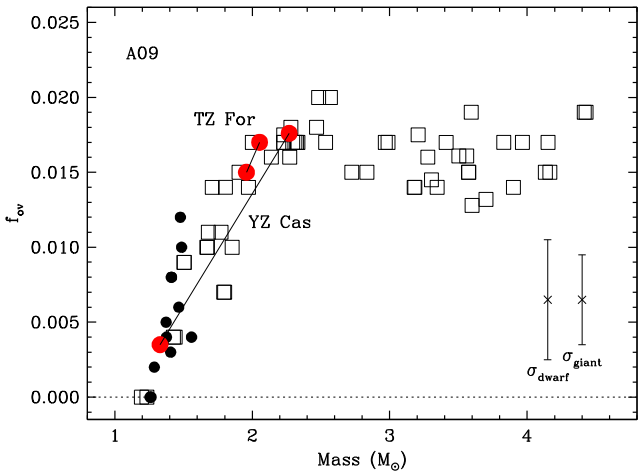

Figure 4. Same as Figure 2 with the f_{ov} values for TZ For and YZ Cas highlighted, and the primary and secondary components in each system connected with a line.

anomalous). Additionally, the ages of the components were found to be very different (420 and 670 Myr), at least for the one model for which details were provided.

Our fits with MESA that allow for independent f_{ov} and α_{MLT} values for the components still point to a somewhat lower abundance than measured, but give essentially the same age for the stars, and f_{ov} values that are consistent with the general trend of Figure 2. Similar results were obtained with the GS98 and A09 mixtures, which we list in Table 2. However, the mixing length parameter values for the secondary (α_{MLT} ~ 2.7) appear implausibly large for a star of this temperature and log g, and are well outside the range found from the 3-D simulations by Magic et al. (2015). Much more reasonable α_{MLT} values were found using the Granada code, which does not account for microscopic diffusion and treats overshooting in the step-function approximation. The ages are still very similar, although the lower inferred value of Z persists with both GS98 and A09, if somewhat improved. While these fits make the situation better in some respects, we consider them to be very provisional pending a better understanding of the remaining discrepancies. For completeness we list the inferred parameters from the Granada fits in Table 2, where for comparison purposes we have converted the original α_{ov} values (0.20 and 0.04 for the primary and secondary, for both mixtures) to f_{ov} values by means of the scaling constant α_{ov}/f_{ov} = 11.36 (see Section 3). These f_{ov} values along with those for TZ For are highlighted in Figure 4.

4.3. OGLE-LMC-ECL-15260 Revisited

The evolved components in this DLEB have essentially the same mass (1.426 ± 0.022 and 1.440 ± 0.024 $M_\odot$) but different radii of 42.17 ± 0.33 and 23.61 ± 0.69 $R_\odot$ for the primary and secondary, respectively (Pietrzyński et al. 2013). The best fits presented in Paper II with the GS98 and A09 element mixtures placed both components on the ascending giant branch, and gave reasonable matches to their properties. A closer look has revealed that a somewhat better match can be found with the two components in the blue loop, a more advanced stage of evolution than we had considered before (see Figure 3), which is slower and a priori more likely.

With the GS98 mixture the inferred f_{ov} and α_{MLT} parameters are only slightly altered relative to the ones in Paper II (and are consistent within the uncertainties). More importantly, the best-fit metal content Z = 0.006 is now in much better agreement with the spectroscopically measured metallicity of OGLE-LMC-ECL-15260 (corresponding to Z = 0.0064), whereas previously our best fit gave Z = 0.003. [4] The change is due in part to our use here of a different enrichment law than in Paper II[5]. With the A09 mixture we again find a good fit for identical f_{ov} values as in Paper II, and only a small increase in the primary α_{MLT} from 2.00 to 2.08 (< 1σ). There is a somewhat more significant decrease in the α_{MLT} value for the secondary from 2.25 to 2.08, which brings it into better agreement with results from 3-D simulations by Magic et al. (2015). As before, the best-fit Z value of 0.004 is consistent with the spectroscopically measured abundance, which is Z = 0.0045 for the A09 mixture. In both of these fits the predicted ages of the primary and secondary are well within 5% of each other, which meets our requirement (c.f. Section 3). The revised parameters are listed in Table 2. For the reasons just described we consider the new solution for OGLE-LMC-ECL-15260 proposed here, with both components in the blue loop, to be preferable to the one reported in Paper II. The f_{ov} values for the A09 mixture are unchanged, and those for GS98 remain perfectly consistent with the general trend of f_{ov} versus mass.

5. CONCLUDING REMARKS

This paper continues our work to investigate the dependence of convective core overshooting on stellar mass, based on a comparison of current stellar evolution models with the best available observations of eclipsing binary systems sufficiently evolved to be useful for this purpose. Treating overshooting as a diffusive process (Freytag et al. 1996; Herwig et al. 1997), we showed in Paper II that the free overshooting parameter f_{ov} increases rapidly from about 1.2 $M_\odot$ to about 2.0 $M_\odot$, flattening thereafter. This result is independent of the element mixture adopted (GS98 or A09). Here we have added 8 new binary systems to the sample studied in Paper II, designed to improve the coverage in the most important mass regime below about 2 $M_\odot$, where f_{ov} is changing the most as mass increases. The new objects nearly double the number available earlier in this mass range, adding 15 individual binary components to the 18 we had before. We have analyzed them with the same methodology used in our previous work, and they fully support the trend reported there.

Six of the added systems belong to a group of stars in the narrow mass range 1.2–1.6 $M_\odot$ that had resisted previous attempts to match their properties at a single age with publicly available stellar evolution models (Clausen et al. 2010; Torres et al. 2014). These models generally offer little or no flexibility to tune the overshooting parameter, whose dependence on mass is "hard-wired" based on various ad-hoc assumptions or theoretical expectations. By allowing f_{ov} to differ between the components we have succeeded in achieving satisfactory

[4] Note that diffusion has a negligible effect for this pair of giant stars.

[5] In that work Y_p and $\Delta Y/\Delta Z$ had been chosen to match our earlier study in Paper I, and enable a proper comparison between f_{ov} and the α_{ov} values of Paper I.

fits. This supports our suspicion that this was at the root of the problem, given that all of these stars happen to be on the steep part of the f_{ov} vs. mass relation. However, one of our original targets in this group, AQ Ser, remains a challenge. We speculate this may be due to the rapid rotation of the components, or perhaps measurement errors in some of its properties. A re-examination of those properties would be helpful.

The YZ Cas system offers a unique opportunity to check the f_{ov} vs. mass relation within the same binary, given that the very different masses of the components happen to be on either side of the 2 $M_{\odot}$ bending point. We find excellent agreement between the f_{ov} values we infer from our model fits and the trend defined by the other DLEBs. However, YZ Cas is not without its problems. Our fits with the MESA code yield unrealistically high α_{MLT} values for the secondary star. The difficulty seems to disappear when using the Granada models, which do not account for diffusion and have a different prescription for overshooting. YZ Cas would benefit from further study to understand the discrepancies, including perhaps a check on the measured properties.

Finally, we have revised the solution in Paper II for OGLE-LMC-ECL-15260 and found a more satisfactory fit with nearly the same f_{ov} values as before that places both components in the blue loop rather than on the ascending giant branch, a more likely stage of evolution.

We are grateful to A. Dotter for his assistance in using the MESA module and for helpful discussions about stellar models. We also thank the anonymous referee, who provided good suggestions for improving the manuscript. The Spanish MEC (AYA2015-71718-R and ESP2017-87676-C5-2-R) is gratefully acknowledged for its support during the development of this work. GT acknowledges partial support from the NSF through grant AST-1509375. This research has made use of the SIMBAD database, operated at the CDS, Strasbourg, France, and of NASA's Astrophysics Data System Abstract Service.

REFERENCES

Ade, P. A. R., Aghanim, N., Arnaud, M. et al. 2016, A&A, 594, A13
Aerts, C. 2013, in Setting a New Standard in the Analysis of Binary Stars, eds. K. Pavlovski, A. Tkachenko & G. Torres, EAS Publications Series, Vol. 64, 2013, pp. 323-330
Andersen, J., Clausen, J. V., Nordstr¨om, B., Tomkin, J., & Mayor, M. 1991, A&A, 246, 99
Asplund, M., Grevesse, N., Sauval, A. J., & Scott, P. 2009, ARA&A, 47, 481 (A09)
B¨ohm-Vitense, E. 1958, ZAp, 46, 108
Claret, A., Gim´enez, A. 1993, A&A, 287, 487
Claret, A. 2004, A&A, 424, 919
Claret, A. 2007, A&A, 475, 1019
Claret, A., Gim´enez, A. 2010, A&A, 519, 57
Claret, A., Torres, G. 2016, A&A, 592, A15 (Paper I)
Claret, A., Torres, G. 2017, ApJ, 849, 15 (Paper II)
Clausen, J. V. 1991, A&A, 246, 397
Clausen, J. V., Frandsen, S., Bruntt, H. et al. 2010, A&A, 516, A42
Deheuvels, S., Brandao, I., Silva Aguirre, V., et al. 2016, A&A, 589A, 93D.
Dotter, A., Conroy, C., Cargile, P., & Asplund, M. 2017, ApJ, 840, 99
Freytag, B., Ludwig, H.-G., & Steffen, M. 1996, A&A, 313, 497
Gallenne, A., Pietrzy´ nski, G., Graczyk, D. et al. 2016, A&A, 586, 35
Grevesse, N., & Sauval, A. J. 1998, Space Sci. Rev., 85, 161 (GS98)
Herwig, F., Bloecker, T., Schoenberner, D., & El Eid, M. 1997, A&A, 324, L81
Lacy, C. H., & Frueh, M. L. 1987, AJ, 94, 712
Lacy, C. H. S., Torres, G., Fekel, F. C., Sabby, J. A., & Claret, A. 2012, AJ, 143, 129
Lacy, C. H. S., Torres, G., & Claret, A. 2008, AJ, 135, 1757
Sandberg Lacy, C. H., Torres, G., Claret, A., Charbonneau, D., O'Donovan, F. T., & Mandushev, G. 2010, AJ, 139, 2347
Magic, Z. Serenelli, A., Weiss, A. et al. 2010, ApJ, 718, 1378
Magic, Z., Weiss, A., & Asplund, M. 2015, A&A, 573, A89
Meng, Y., & Zhang, Q. S. 2014, ApJ, 787, 127
Michaud, G. 1970, ApJ, 160, 641
Michaud, G., Charland, Y., Vauclair, S., & Vauclair, G. 1976, ApJ, 210, 447
Moravveji, E., Townsend, R. H. D., Aerts, C., & Mathis, S. 2016, ApJ, 823, 130
Pavlovski, K., Southworth, J., Kolbas, V., & Smalley, B. 2014, MNRAS, 438, 590
Paxton, B., Bildsten, L., Dotter, A. et al. 2011, ApJS, 192, 3
Paxton, B., Cantiello, M., Arras, P., et al. 2013, ApJS, 208, 4
Paxton, B., Marchant, P., Schwab, J., et al. 2015, ApJS, 220, 15
Pedersen, M. G., Aerts, C., P´apics, P. I., & Rogers, T. M. 2018, A&A, in press (arXiv:1802.02051)
Pietrzy´nski, G., Graczyk, D., Gieren, W. et al. 2013, Nature, 495, 76
Reimers, D. 1977, A&A, 61, 217
Ribas, I., Jordi, C., & Gim´enez, A. 2000, MNRAS, 318, 55
Stancliffe, R. J., Fossati, L., Passy, J.-C., & Schneider, F. R. N. 2015, A&A, 575, 117
Torres, G., Andersen, J., & Gim´enez, A. 2010, A&A Rev., 18, 67
Torres, G., Claret, A., Pavlovski, K., & Dotter, A. 2015, ApJ, 807, 26
Torres, G., Vaz, L. P. R., Lacy, C. H. S., & Claret, A. 2014, AJ, 147, 36
Valle, G., Dell'Omodarme, M., Prada Moroni, P. G., & Degl'Innocenti, S. 2016, A&A, 587, 16
Valle, G., Dell'Omodarme, M., Prada Moroni, P. G., & Degl'Innocenti, S. 2017, A&A, 600, A41